

*[Reprinted from THE AERONAUTICAL JOURNAL OF THE ROYAL AERONAUTICAL SOCIETY, JULY 2001]*

# Optimisation of aero gas turbine engines

**A. Guha**

Aerospace Engineering Department  
University of Bristol  
Bristol, UK



# Optimisation of aero gas turbine engines

A. Guha

Aerospace Engineering Department

University of Bristol

Bristol, UK

## ABSTRACT

A systematic methodology for the thermodynamic optimisation of civil bypass engines (turbofan or advanced propulsors) is presented, which would be useful for designing air-breathing engines based on "clean-sheet analysis". The process starts with establishing an optimum specific thrust for the engine based on an economic analysis (installation constraints, noise regulations etc. also need to be considered). The task of the optimisation process is then to find the combination of optimum values of fan pressure ratio, overall pressure ratio, bypass ratio and turbine entry temperature concurrently that maximises overall efficiency at the fixed specific thrust. This procedure is quite different from the usual single-variable parametric performance studies which do not give proper optimum values and may involve large excursion in the value of the specific thrust unacceptable for a particular mission. Additionally, several, simple and explicit, analytical relations are derived here from fundamental principles, which perform well against numerical optimisation performed by a specialist computer program employing iterative and advanced search techniques. The analytical relations accelerate the optimisation process and offer physical insight. Present numerical computations with real gas properties have established new concepts in turbofan optimisation (for example, the existence of an optimum bypass ratio and optimum turbine entry temperature). The question of optimum jet velocity has been addressed. An analytical expression for the optimum jet velocity at a given bypass ratio has been derived which performs well against numerical optimisation results.

## NOMENCLATURE

$B$	bypass ratio, $B = \dot{m}_c / \dot{m}_h$
$c_p$	specific heat of air at constant pressure
$D$	drag
$E_k$	kinetic energy added by the core engine
$f$	fuel-air ratio by mass, $f = \dot{m}_f / \dot{m}$
$f_h$	fuel-air ratio by mass based on the core engine, $f_h = \dot{m}_f / \dot{m}_h$
$F_N$	net thrust
$\hat{F}_N$	specific thrust, $\hat{F}_N = F_N / \dot{m}$
$FPR$	fan pressure ratio
$g$	acceleration due to gravity
$L$	lift
$\dot{m}$	total mass flow rate of air, $\dot{m} = \dot{m}_h + \dot{m}_c$

$\dot{m}_c$	mass flow rate through the bypass duct (cold flow)
$\dot{m}_f$	mass flow rate of fuel
$\dot{m}_h$	mass flow rate of air through the core engine (hot flow)
$M$	Mach number of the aircraft
$OPR$	overall pressure ratio
$p$	static pressure
$p_0$	total pressure
$Q_{cv}$	lower calorific value of fuel
$R$	specific gas constant of air
$R_a$	range of aircraft
$sfc$	specific fuel consumption, $sfc = \dot{m}_f / F_N$
$T$	static temperature
$T_a$	temperature of ambient air
$T_0$	total temperature
$V$	velocity
$V_a$	forward speed of the aircraft
$V_{jc}$	fully expanded jet speed of the cold bypass stream
$V_{jh}$	fully expanded jet speed of the hot core stream
$V_{j,ref}$	jet speed in the reference turbojet engine, Fig. 2
$V_m$	mean jet speed, (Equation (8))
$\gamma$	isentropic index of air
$\eta_{core}$	thermal efficiency of the core engine (Equation (21))
$\eta_f$	isentropic efficiency of the fan
$\eta_{KE}$	efficiency of energy transfer between the core and bypass flow
$\eta_{LPT}$	isentropic efficiency of the low pressure turbine
$\eta_{NB}$	isentropic efficiency of the bypass nozzle
$\eta_0$	overall efficiency of the whole engine
$\eta_P$	propulsive efficiency of the whole engine
$\eta_T$	thermal efficiency of the whole engine, (Equation (21))
$\mathfrak{R}$	mean jet speed ratio, $\mathfrak{R} = V_m / V_a$

## Subscripts

$op$	optimum value
2	before the fan
4	entry to high pressure turbine
13	after the fan in bypass stream

## 1.0 INTRODUCTION

Turbofan engines are currently the prime choice for subsonic civil air transport. The economic drive to improve fuel burn might lead to future turbofan engines with lower specific thrust and large bypass ratios or even novel engine configurations<sup>(1,2)</sup>. Performance analysis of turbofan engines is discussed in details in several excellent texts (Hill and Peterson<sup>(3)</sup>, Cohen *et al.*<sup>(4)</sup>, Cumpsty<sup>(5)</sup>). Mattingly<sup>(6)</sup> has provided extensive theoretical coverage on parametric cycle analysis (pp 240-460), whereas Walsh and Fletcher<sup>(7)</sup> cover a wide range of practical issues (they also provide parametric performance curves, pp 361-381). In comparison to the treatment of gas turbine performance in a large number of available texts, the issue of optimised design has received little attention, and theoretical solutions did not exist. The issue is complex because, other than several design constraints, there are a large number of variables involved. However, a good deal about the overall features of an engine can be described by the specific thrust ( $\dot{F}_N$ ) and the specific fuel consumption ( $sfc$ ), and the designer has to determine four main input variables: the overall pressure ratio ( $OPR$ ), the turbine entry temperature ( $T_{04}$ ), the bypass ratio ( $B$ ) and the fan pressure ratio ( $FPR$ ).

In this paper a new methodology for the optimisation of jet engines has been formulated in which the optimum combination of all variables is determined concurrently that maximises the overall efficiency while maintaining the specific thrust at a predetermined value established from a direct operating cost (DOC) analysis. This is very different from the parametric studies<sup>(3,6,7)</sup> where the effects of the variation of a single variable are calculated numerically while all other variables are kept fixed – therefore at their non-optimum levels. The parametric studies are thus not capable of finding the true optimum combination. Moreover, often such parametric studies may involve a large excursion in the value of the specific thrust which is unacceptable for a particular mission. So, even with the availability of a computational package, the present methodology offers a more logical approach. Additionally, several, simple and explicit, new analytical relations have been derived here that accelerate the optimisation process and offer physical insight. With these, the optimisation can be undertaken with hand calculations at the initial phase of a real design process and can also be treated realistically in a textbook.

A store-house of expertise and knowledge obviously exists with the aero-engine manufacturers who have endeavoured to continuously improve the gas turbine performance for the past 60 years. Meece<sup>(8)</sup> graphically shows the improvement in aircraft fuel efficiency as the seat-mile per US gallon increased from about 40 in 1960 to about 100 in the late 1990s. About half of this progress has been due to engine improvements and the other half due to aircraft improvements. Ruffles<sup>(9)</sup> shows that there has been a 50% improvement in the specific fuel consumption ( $sfc$ ) of the bare engine, as the engines evolved from the turbojet of 1958 (~11bm/hr/lbf) to the likes of high bypass Trent engines of modern time (~0.55lbm/hr/lbf). Improvements in propulsive efficiency, component efficiency and cycle efficiency contribute approximately one-third each to this gain in performance. This improvement has resulted from advances in aerodynamics, combustion and materials offering higher strength and temperature capability combined with better design tools, analysis techniques and manufacturing processes. Applications of non-linear, transient and dynamic finite element analysis (FEA) and computational fluid dynamics (CFD) have improved the design and analysis capability significantly. A steady rise in the turbine entry temperature (TET) has increased the specific power of the core engine by a factor of 5 over the early jet engines of Whittle and von Ohain. Since the 1960s there has been a 75% reduction in aircraft noise. Over the last 25 years, engine reliability as measured by in-flight shutdown rate has improved by more than a factor of 10, largely due to the increased maturity of engine systems, electronic engine controls and increased reliability testing during the development phase<sup>(10)</sup>. Great improvements in engine life, reliability and maintainability have provided significant reduction in life cycle cost.

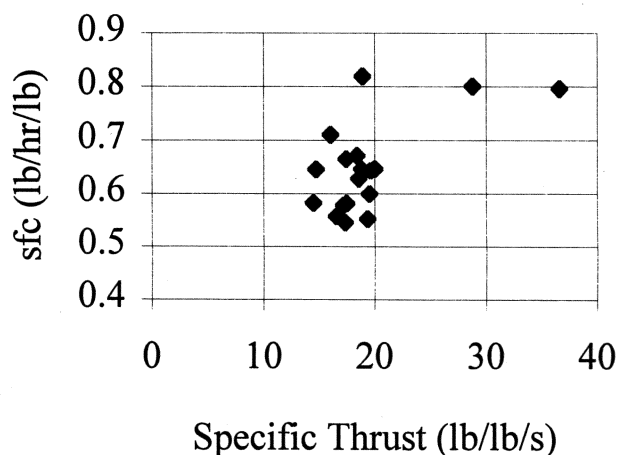


Figure 1. Data for various current civil turbofan engines under cruise conditions (typically 35,000ft,  $M = 0.8-0.85$ ).

The publications made by experts from industry (eg Jackson<sup>(11)</sup>, Bennett<sup>(1)</sup>, Wilde<sup>(12)</sup>) contain a wealth of experience, information and calculation results. However, the details of calculation method or optimisation procedure are not known to the readers. Moreover, the published results would usually involve an adopted family of engine designs. The studies might often be conducted keeping the core engine fixed. It is then not always obvious to the general reader how to generalise the results or how to proceed on a clean-sheet analysis.

In this paper the overall efficiency ( $\eta_0$ ) has been treated as the fundamental quantity in determining fuel economy. The specific fuel consumption is related to the overall efficiency through the equation  $sfc = V_a / (\eta_0 Q_{cv})$ . Thus, at a given forward speed of the aircraft, maximising  $\eta_0$  is synonymous to minimising  $sfc$ . Overall efficiency is often expressed as the product of propulsive efficiency and thermal efficiency ( $\eta_0 = \eta_p \eta_T$ ). Many discourses on gas turbine performance therefore, for the ease of presentation, first discuss the performance of ground-based gas turbines producing shaft power (although historically gas turbine has been first developed as aero engines). The ideal joule cycle, effects of component irreversibilities, effects of  $OPR$  and  $T_{04}$  on the maximum thermal efficiency are then discussed. Then the ideas of jet engine are introduced where, other than the thermal efficiency, propulsive efficiency has also to be considered. However, caution is needed in treating the thermal and propulsive efficiencies separately at least for two reasons.

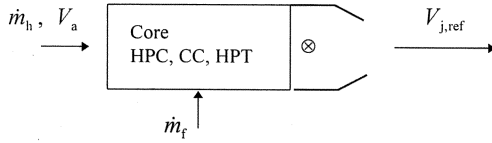
- (i) In a jet engine, unlike ground-based gas turbines, the effect of a single variable on thermal efficiency cannot be considered in isolation because this alters the jet velocity, which, in turn, affects the propulsive efficiency.
- (ii) In the breakdown  $\eta_0 = \eta_p \eta_T$  for a turbofan engine,  $\eta_T$  does not just represent the thermal efficiency of the core engine – the equivalent of the ground-based gas turbine – but also includes the dissipation in the transfer of power from the core to the bypass stream. (Most references seem to ignore this altogether. Equation (21) given later and Appendix I show that the impact of this factor cannot be neglected particularly at high bypass ratios.)

Here specific thrust has been treated as the basic design parameter. The specific thrust is a good overall indicator of the engine for the following reasons:

- (i) It fixes the mean jet speed (Equation (9) given later). Thus it determines the propulsive efficiency (Equation (13)); and, governs the jet noise, as the jet noise is approximately proportional to the eighth power of jet speed. Environmental considerations such as the noise level would increasingly determine the design parameters of a future jet engine.



## a. Turbojet



## b. Separate-stream bypass engine

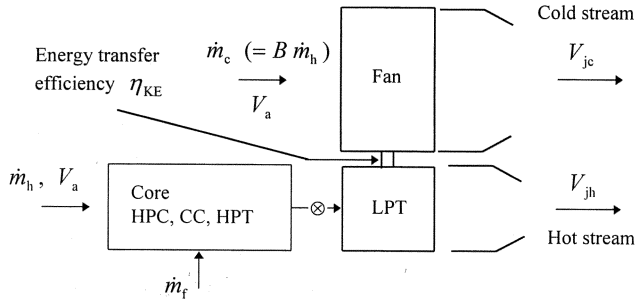


Figure 2. Schematic description of a separate-stream turbofan engine and an equivalent turbojet engine used for analysis. (The energy is the same at point  $\otimes$  in both engines).

- (ii) For a given thrust required, the specific thrust almost fixes the fan diameter and hence the size of the engine.
- (iii) Thus a given value of specific thrust largely determines the nacelle weight, price and drag.
- (iv) The specific thrust determines whether the engine would satisfy any geometric constraint (for example, whether the engine could be fitted under the wing).

In order to establish the relevant range of specific thrust that should be employed in the present theoretical study, the values of the specific thrust<sup>(13)</sup> of several current civil turbofan engines of various manufacturers have been plotted in Fig. 1. Specific thrust data in Fig. 1 are slightly approximate because although net thrust is known at cruise, the mass flow rate is estimated from given values at sea level static conditions by dynamic scaling, ie assuming the same non-dimensional operating point.

Figure 1 shows that for most existing engines, the cruise specific thrust lies in the band 15–20 lbf/lbm/s. Over the past forty years of civil engine design the specific thrust has reduced significantly while the bypass ratio has increased from 1–2 in the 1960s to 7–9 in the 1990s. The trend of reducing specific thrust with time has been accompanied by technology improvements bringing reductions of installation drag and specific weight of engines. The forecast<sup>(2,8,10,14)</sup> is that the design driver for future engines might be towards even lower specific thrust. A surge in fuel price and/or the introduction of more stringent noise regulation may necessitate such designs. Future geared turbofan or advanced ducted propulsors (ADP) would reduce the specific thrust significantly.

Figure 1 also shows the *sfc* of various engines. Detailed data regarding *OPR*, *B*, thrust, configuration, number of stages, date of entry into service etc are given in Ref. 13. The variation in *sfc* reflects the effects of these factors and evolving technology standard. Considerations of engine weight and initial price, stage length of the aircraft, fuel price etc influence design decisions.

Following industrial practice, the *sfc* and the specific thrust have been expressed here respectively in lbf/hr/lbf and lbf/lbm/s. 1 lbf/lbm/s is equal to 9.81 ms<sup>-1</sup>, and 1 lbf/hr/lbf is equal to 28.316  $\leftrightarrow$  10<sup>-6</sup> kg/s/N.

## 2.0 DETERMINATION OF THE OPTIMUM FAN PRESSURE RATIO, (FPR)<sub>OP</sub>

The schematic arrangement and flow structure in a turbofan engine is shown in Fig. 2. The description of an equivalent turbojet engine is also shown in the same figure as a reference point in the analysis.

Let us suppose that the core gas generator produces, for a particular value of fuel consumption rate, a jet with speed  $V_{j,ref}$  in the absence of any bypass flow. The kinetic energy added by the gas generator is then, neglecting the fuel mass flow rate which is usually a very small proportion of the air mass flow rate in a jet engine, equal to

$$E_k = \frac{1}{2} \dot{m}_h (V_{j,ref}^2 - V_a^2) \quad \dots (1)$$

In the bypass engine, the whole of this kinetic energy is, of course, not present in the core jet. The low pressure (LP) turbine extracts a portion of this energy and turns the fan which, in turn, adds kinetic energy to the bypass flow. The efficiency,  $\eta_{KE}$ , of this energy transfer between the core and bypass flow depends on the component efficiencies of the LP turbine, the fan and the bypass nozzle, and also on the flow losses in the ducts and mechanical efficiency of the shafts. Assuming the mechanical efficiency is close to 1,

$$\eta_{KE} \approx \eta_{LPT} \eta_f \eta_{NB} \quad \dots (2)$$

At the current level of technologies<sup>(5,10)</sup>  $\eta_{LPT} \approx 0.9$ ,  $\eta_f \approx 0.9$ ,  $\eta_{NB} \approx 1$ . Equation (2) therefore suggests that  $\eta_{KE} \approx 0.8$ .

In a bypass engine the kinetic energy given by Equation (1) is related to the sum of the kinetic energies of the two streams by,

$$E_k = \frac{1}{2} \dot{m}_h (V_{j,ref}^2 - V_a^2) = \frac{1}{2} \dot{m}_h (V_{jh}^2 - V_a^2) + \frac{1}{2} \dot{m}_c \frac{B}{\eta_{KE}} (V_{jc}^2 - V_a^2) \quad \dots (3)$$

In Equation (3) the mass flow rate of the bypass stream,  $\dot{m}_c$ , has been expressed in terms of  $\dot{m}_h$  and *B*, the bypass ratio.

Similarly the net thrust,  $F_N$ , produced by the bypass engine is given by,

$$F_N = \dot{m}_h (V_{jh} - V_a) + B \dot{m}_h (V_{jc} - V_a) \quad \dots (4)$$

The pressure thrust has been taken into account because  $V_{jh}$  and  $V_{jc}$  are the fully-expanded jet velocities of the two streams.

The objective of the optimisation process is to determine the ratio  $V_{jc}/V_{jh}$  which would maximise the net thrust  $F_N$ , while keeping the fuel consumption fixed.

The condition for maximum net thrust is given by,

$$\frac{\partial F_N}{\partial V_{jh}} = 0 \quad \dots (5)$$

At constant thermal efficiency, a fixed fuel consumption means  $E_k$  in Equation (3) is constant. Therefore,

$$\frac{\partial (E_k)}{\partial V_{jh}} = 0 \quad \dots (6)$$

For a constant bypass ratio, *B*, Equations (3), (4), (5) and (6) can be combined to give,

$$\left( \frac{V_{jc}}{V_{jh}} \right)_{op} = \eta_{KE} \quad \dots (7)$$

While evaluating the partial derivatives in Equations (5) and (6),

$B$  and  $\dot{m}_h$  are assumed constant. Together they specify a constant inlet air flow. Since the specific thrust is the ratio of net thrust and mass flow rate of air at inlet, Equation (5) is also the condition for maximum specific thrust. Specific fuel consumption is the ratio of mass flow rate of fuel and net thrust. Equation (6) implies a fixed mass flow rate of fuel, Equation (5) is thus also the condition for minimum specific fuel consumption. Since Equation (7) gives both maximum specific thrust and minimum specific fuel consumption, this condition has been used in the analytical formulation of the optimisation process that follows.

A designer can satisfy Equation (7) in a real engine by choosing the optimum fan pressure ratio,  $(FPR)_{op}$ , as shown below. The choice of the specific thrust,  $\hat{F}_N$ , and the bypass ratio,  $B$ , as the independent variables becomes helpful in this respect because  $(FPR)_{op}$  can be expressed as an explicit algebraic function of  $\hat{F}_N$  and  $B$ .

The mean jet speed  $V_m$  can be expressed, using Equation (7), as

$$V_m = \frac{1}{1+B} \left[ B + \frac{1}{\eta_{KE}} \right] V_{jc} \quad \dots (8)$$

and it follows that,

$$\hat{F}_N = \frac{F_N}{\dot{m}_h + \dot{m}_c} = V_m - V_a \quad \dots (9)$$

Suppose the rise in total temperature in the bypass flow for a hypothetical, isentropic compression by the fan, for the same pressure ratio that exists across a real fan, is  $\Delta T_{0, isen}$ . If the fan and the bypass nozzle were isentropic, then the static temperature of the fully expanded jet would be equal to the ambient temperature. Application of the steady flow energy equation then gives,

$$\Delta T_{0, isen} = \frac{1}{2c_p} (V_{jc}^2 - V_a^2) \quad \dots (10)$$

Equations (8), (9) and (10) can be combined with the isentropic pressure-temperature relation. One then obtains, after some algebraic manipulation, the final expression for the optimum fan pressure ratio:

$$(FPR)_{op}^{\frac{\gamma-1}{\gamma}} = 1 + \frac{(\gamma-1)}{2+(\gamma-1)M^2} \left[ \frac{(1+B)^2}{(B+1/\eta_{KE})^2} \left\{ \frac{\hat{F}_N}{\sqrt{\gamma R T_a}} + M \right\}^2 - M^2 \right] \quad \dots (11)$$

All quantities in Equation (11) are non-dimensional numbers. Figure 3 shows graphically the prediction of Equation (11).

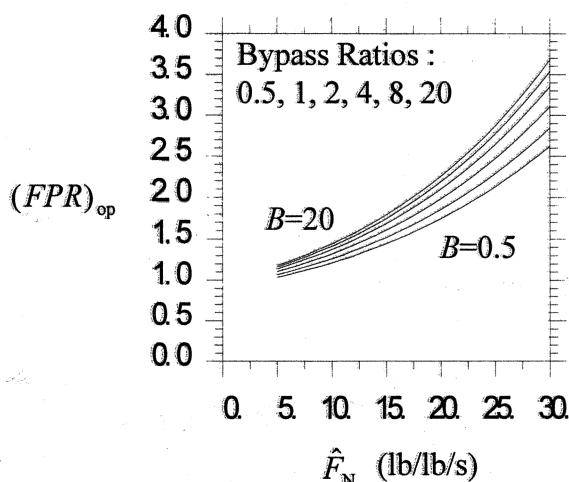


Figure 3. Variation of optimum fan pressure ratio with specific thrust: prediction of Equation (11). ( $M = 0.82$ ,  $T_a = 216.65K$ ,  $\eta_{KE} = 0.81$ ,  $\gamma = 1.4$ ).

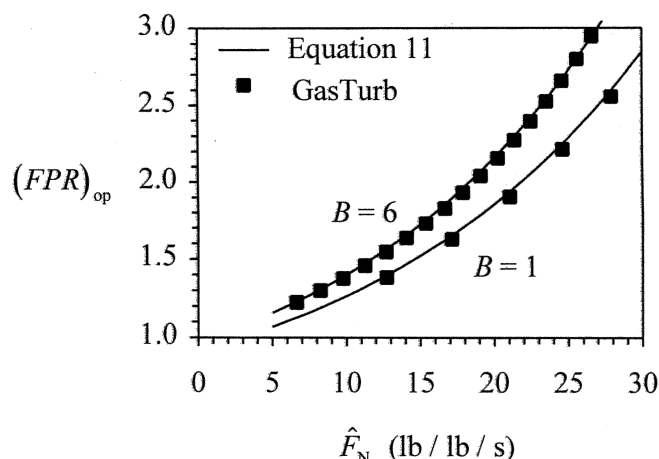


Figure 4. Comparison of present theory with numerical optimisation results for optimum fan pressure ratio. (Altitude = 11km,  $M = 0.82$ , isentropic efficiency of compressors and turbines = 0.9).

One interesting feature of Equation (11) is that if  $\eta_{KE} = 1$  (ie in the case of ideal energy transfer from the core stream to the bypass stream) the bypass ratio  $B$  drops out of the equation.  $(FPR)_{op}$  would then have depended only on  $\hat{F}_N$ . At any rate, Equation (11) predicts that, for a fixed  $\hat{F}_N$ , the dependence of  $(FPR)_{op}$  on  $B$  is weak, especially at higher values of  $B$  ( $B > 4$ ). Equation (11) also produces the expected limiting result:

$$Lt (FPR)_{op} = 1.$$

$$B \rightarrow \infty$$

$$\hat{F}_N \rightarrow 0$$

For a chosen specific thrust  $\hat{F}_N$  and bypass ratio  $B$ , Equation (11) immediately specifies the optimum fan pressure ratio. The design wisdom is that only a single stage fan is used for a civil aircraft engine, the maximum  $FPR$  is therefore restricted to 1.8. (Military engines with low bypass ratio normally uses an LP compressor having a maximum of 3-4 stages.) A limit of minimum  $FPR$  may also arise due to fan instabilities at partload, off-design conditions. According to Rüd and Lichtfuss<sup>(2)</sup>, below an  $FPR$  of 1.4, the engine will require variable geometry either via a variable pitch fan or a variable area bypass nozzle in order to provide aerodynamic fan stability under partload conditions. Therefore, knowing  $(FPR)_{op}$  at an early stage of the design is an advantage. If its value does not lie within the desired limit, the choice of  $\hat{F}_N$  and  $B$  can be altered (of course, another option would be not to adhere strictly to the optimum value of  $FPR$ ).

Equation (11) has been tested against optimisation performed by the computer program GasTurb<sup>(15)</sup> which is a general purpose commercial package for the calculation of design and off-design performance of various types of gas turbine engines – turbojet, turboshaft, separate or mixed stream turbofan, geared turbofan, with single or twin-spool configurations. It has several features including optimisation, iteration, transient and Monte Carlo simulation. Figure 4 shows the comparison of the present theory with numerical optimisation. Each numerical point has been calculated by GasTurb by a lengthy optimisation process which uses advanced search techniques to find the optimum  $FPR$  that minimises the specific fuel consumption while, at each trial, the primary variables are iterated to give the prescribed specific thrust. Figure 4 shows that Equation (11) performs well against sophisticated numerical optimisation, and can, therefore, be used for the design of real engines. Equation (11) has not previously appeared in the literature. (The numerical calculations are performed in the range  $OPR = 20-40$ , and it is found that any combination of  $OPR$  and  $T_{04}$ , while  $\hat{F}_N$  and  $B$  are kept fixed, produces essentially the same value of  $(FPR)_{op}$ . This is predicted by Equation (11)).

Bypass ratio	$(V_{jc}/V_{jh})_{op}$ Numerical optimisation with GasTurb	$(V_{jc}/V_{jh})_{op} = \eta_{KE}$ ( $\eta_{KE} \approx \eta_{LPT} \eta_f \eta_{NB}$ )
1	0.808	0.81
3	0.791	0.81
6	0.794	0.81

Table 1

Comparison of theory and numerical results for optimum  $V_{jc}/V_{jh}$ 

Equation (7) shows that there is a particular ratio of the fully expanded jet velocities of the cold and hot stream ( $(V_{jc}/V_{jh})_{op} = \eta_{KE}$ ) that simultaneously achieves minimum specific fuel consumption and maximum specific thrust. The designer can make the two jet velocities take this value by choosing the optimum fan pressure ratio.

The computational program GasTurb was used to find the ratio  $V_{jc}/V_{jh}$  that occurs in an engine whose *FPR* has been numerically optimised for minimising *sfc*. Table 1 shows these values (for  $OPR = 30$ ,  $T_{04} = 1,200\text{K}$ ,  $\eta_{LPT} = 0.9$ ,  $\eta_f = 0.9$ ,  $\eta_{NB} = 1$ ), against the prediction of Equation (7).

Numerical optimisations were performed at several other *OPR* and  $T_{04}$ :  $V_{jc}/V_{jh}$  lay between 0.77 and 0.82 (for the assumed component efficiencies). The numerical calculations show that the derived analytical relation, Equation (7), is approximately valid.

In this section only the separate-stream engines have been considered. The analytical and numerical determination of optimum fan pressure in mixed-stream engines, in which the core and bypass flow are mixed and then exhausted through a common nozzle, has been described by Guha elsewhere<sup>(16)</sup>. There it is shown that at the same specific thrust and bypass ratio, the optimum fan pressure ratio for a mixed-stream engine is lower than that of a separate-stream engine. For mixed-stream engines, the dependence of  $(FPR)_{op}$  on bypass ratio is very weak, and  $(FPR)_{op}$  also depends on overall pressure ratio.

### 3.0 DETERMINATION OF OPTIMUM JET SPEED, $(V_m/V_a)_{op}$

The purpose of this section is to determine the relation between the mean jet speed and aircraft speed for maximum fuel economy. It appears that the question of optimum jet speed has not been addressed to any great extent in the literature. Before presenting the new result, it would be worth briefly re-examining some basic concepts. This would serve to set the background, as rather subtle issues are involved.

Equation (4) can be rewritten in terms of the mean fully-expanded jet velocity  $V_m$ ,

$$F_N = \dot{m} (V_m - V_a) \quad \dots (12)$$

where, the total mass flow rate of air,  $\dot{m}$ , is given by  $\dot{m} = \dot{m}_h + \dot{m}_c$ .

The propulsive efficiency  $\eta_p$  is given by,

$$\eta_p = \frac{V_a}{V_a + \frac{1}{2}(V_m - V_a)} = \frac{1}{1 + \frac{1}{2}(\hat{F}_N/V_a)} \quad \dots (13)$$

Equation (12) shows that the same thrust can be obtained either by a large mass flow rate and a small velocity increase, or, a small mass flow rate and a large velocity increase. A propeller uses the first option, a turbojet engine uses the second. Equation (13) shows that for maximum propulsive efficiency, the jet speed should be as close to the aircraft speed as possible. Of course, practical limitations concerning the engine size would prohibit the attainment of this

limiting jet velocity, but wider considerations show that this is not even desirable from the fuel economy point of view.

For a civil transport, aircraft range,  $R_a$ , is a crucial parameter indicating fuel economy. Breguet's formula shows that,

$$R_a = \eta_0 \left( \frac{L}{D} \right) \left( \frac{Q_{cv}}{g} \right) \ln \left( \frac{m_{initial}}{m_{final}} \right) \quad \dots (14)$$

Equation (14) shows that the range depends on the overall efficiency  $\eta_0$  of the engine and the  $(L/D)$  characteristic of the whole aircraft. It is the overall efficiency, therefore, which needs to be maximised for best fuel economy.

The overall efficiency  $\eta_0$  can be expressed as,

$$\eta_0 = \frac{(V_m - V_a)V_a}{f Q_{cv}} \quad \dots (15)$$

For the best choice of the ratio  $V_m/V_a$ , set  $\partial\eta_0/\partial V_a = 0$ . This gives, for maximum  $\eta_0$ ,

$$(V_m/V_a)_{op} = 2 \quad \dots (15a)$$

This calculation (Hill and Peterson<sup>(3)</sup>, p 152) is illustrative because this shows that the consideration of propulsive efficiency alone had got this ratio inappropriate by a factor of 2 (see the discussion after Equation 13 which shows that for maximum propulsive efficiency,  $(V_m/V_a) \sim 1$ ).

This analytical result for optimum jet velocity ratio,  $(V_m/V_a)_{op} = 2$ , might work reasonably well for subsonic, pure turbojet (which would have been quite a wrong choice, in the first place, if fuel economy were a major concern). However, this relation does not hold for supersonic pure turbojets.

The subtle reason is that while employing the condition  $\partial\eta_0/\partial V_a = 0$ , one has assumed that for a given  $f$ ,  $V_m$  does not depend on  $V_a$ . This is not quite true because of two reasons: (i) the ram effect and (ii) intake losses, both of which depend on the inlet Mach number, becoming increasingly important as the Mach number rises. Moreover, it turns out that the optimum jet speed ratio obtained by keeping  $V_a$  fixed and letting  $V_m$  to vary is not quite the same as that obtained by keeping  $V_m$  fixed and letting  $V_a$  to vary. The latter maximises  $\eta_0$  ( $V_a/\text{sfc}$ ), while the former effectively minimises *sfc* since  $V_a$  is constant. Table 2 shows this point.

It may be noted from Table 2 that the two optimisation processes produce different  $(V_m/V_a)_{op}$ . For Case 1 operating condition, the *sfc* is lower; but the overall efficiency is higher in Case 2. The  $(L/D)$  ratio of the aircraft at  $M = 1.069$  would, however, be poor. Equation (14) then shows that the aircraft range would be poor.

It has been argued (Hill and Peterson<sup>(3)</sup>, p 153; Smith<sup>(17)</sup>) that the condition  $(V_m/V_a)_{op} = 2$  holds for turbofan engines as well. This conclusion makes one uneasy because intuitively one expects that  $(V_m/V_a)_{op}$  should tend to unity as  $B \rightarrow \infty$ , recovering the result

Table 2  
Numerical determination of optimum  $V_m/V_a$  for a pure turbojet in two different ways

	OPR	TET $T_{04}(\text{K})$	M	$(V_m/V_a)_{op}$	sfc (lb/hr/lb)	$\eta_p$	$\eta_0$
Case 1	29.83	913.5	0.816	2.27	0.7043	0.6145	0.2799
Case 2	29.83	913.5	1.069	1.64	0.8287	0.7602	0.3116

Case 1: At a fixed Mach number 0.816 and *OPR*,  $T_{04}$  was allowed to vary freely to maximise  $\eta_0$ .

Case 2: At fixed *OPR* and  $T_{04}$ , obtained in the previous optimisation process, the aircraft Mach number *M* was allowed to vary freely to maximise  $\eta_0$ .

obtained by considerations of propulsive efficiency alone. The following analysis resolves this paradox.

The explanation again lies in the fact that the relation  $(V_m/V_a)_{op} = 2$  would be true if for a given  $f$ ,  $V_m$  did not depend on  $V_a$ . The latter condition does not hold for a turbofan engine, even at subsonic aircraft speeds.

In order to appreciate this point, Equation (15) is rewritten in terms of  $V_{j,ref}$  by employing Equations (3), (7), (8) and (12). After some algebraic manipulations, the final result can be expressed as,

$$\eta_0 = \frac{\left[ \sqrt{1+B\eta_{KE}} \sqrt{V_{j,ref}^2 + (B/\eta_{KE})V_a^2} - (1+B)V_a \right] V_a}{f_h Q_{cv}} \quad \dots (16)$$

For maximum  $\eta_0$ ,

$$\frac{\partial \eta_0}{\partial V_a} = 0 \quad \dots (17)$$

For a particular value of  $B$ , Equations (16) and (17) give,

$$\mathfrak{R}_{op} \equiv \left( \frac{V_m}{V_a} \right)_{op} = 1 + \sqrt{1 - \frac{B(B+1/\eta_{KE})}{(1+B)^2}} \quad \dots (18)$$

The optimal jet speed ratio,  $\mathfrak{R}_{op}$ , given by Equation (18), behaves properly in both limits. For example, as  $B \rightarrow 0$ ,  $\mathfrak{R}_{op} \rightarrow 2$ , thus recovering the pure turbojet result. As  $B \rightarrow \infty$ , Equation (18) shows that  $\mathfrak{R}_{op} \rightarrow 1$ , as is anticipated for a turbofan engine with an extremely large bypass ratio.

From Equation (18), one can immediately write,

$$\left( \frac{V_{j,ref}}{V_a} \right)_{op} = \sqrt{\frac{\{(1+B)\mathfrak{R}_{op}\}^2}{1+B\eta_{KE}} - \frac{B}{\eta_{KE}}} \quad \dots (19)$$

$$\left( \frac{\hat{F}_N}{V_a} \right)_{op} = \mathfrak{R}_{op} - 1 = \sqrt{1 - \frac{B(B+1/\eta_{KE})}{(1+B)^2}} \quad \dots (20)$$

Though  $(V_m/V_a)_{op}$  decreases with increasing bypass ratio as per Equation (18), Equation (19) shows that  $(V_{j,ref}/V_a)_{op}$  rises monotonically with increasing bypass ratio. This means the optimum  $T_{04}$  rises with increasing bypass ratio (since  $V_{j,ref}$  is a measure of the total energy added as a result of the burning of fuel). Equation (20) defines the optimum specific thrust, at a particular bypass ratio  $B$ , for maximum overall efficiency (hence minimum  $sfc$  at a particular aircraft speed). Equation (20) thus shows that, for a specific  $B$ , there is no point in reducing the specific thrust any below its optimum value. Any further reduction in specific thrust would make the fuel consumption rise: this conclusion is not intuitively obvious.

Figure 5 shows the comparison of Equation (18) with numerical computations by GasTurb which uses real gas properties including equilibrium dissociation. It is recalled that previous theories predicted a constant value of 2 for  $(V_m/V_a)_{op}$  at all bypass ratios.

#### 4.0 DETERMINATION OF OPTIMUM BYPASS RATIO, $B_{OP}$ , FOR A GIVEN SPECIFIC THRUST

The bypass ratio controls the relative size of the core engine with respect to the overall engine, affects the number of LP turbine stages, and determines whether or not a gear drive may be necessary. Dependence of many parameters (e.g. fan diameter, propulsive efficiency, jet noise and nacelle drag) are often ascribed to bypass ratio in the literature, though these parameters are fundamentally related

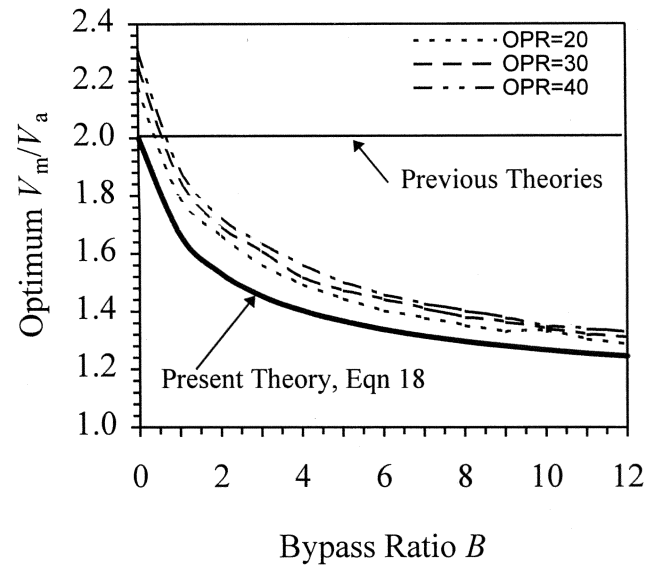


Figure 5. Comparison of analytical results with numerical optimisation for optimum jet speed. (The dashed lines are obtained by numerical optimisation. For this, at each bypass ratio and fixed  $OPR$ ,  $T_{04}$  and  $FPR$  were varied until the overall efficiency  $\eta_0$  was maximised. For all calculations, altitude = 11km,  $M = 0.82$ , isentropic compressor and turbine efficiencies 0.9.)

to specific thrust. It is only for a fixed core engine that the variation in design bypass ratio would be uniquely related to that in the design specific thrust. For a given engine, bypass ratio varies at different operating points.

Cumpsty<sup>(5)</sup> (p 72) reports that there are disagreements among the leading engine manufacturers about the choice of bypass ratio. His calculation (his Fig. 7.4) shows that the  $sfc$  monotonically decreases with increasing bypass ratio in an uninstalled engine. When these calculations were modified by accounting for the increased nacelle drag by an empirical formula [ $sfc_{installed} = \{1.04 + 0.01(B-1)\}sfc_{bare}$ ], the advantages at higher bypass ratios diminished but nevertheless the  $sfc$  continued to decrease monotonically with increasing bypass ratio. However, when other considerations such as engine weight, size, cost, and, provision of gear box and noise level are considered, there is scope to apply individual judgement of the designer.

The above conclusions result from working with variables like  $OPR$  and  $T_{04}$ , or, in other words, in trying to keep the same core engine. It has already been argued that the logical starting point should be the specific thrust. At a fixed specific thrust, the nacelle diameter virtually remains fixed, and so does its weight, cost, and drag. One can therefore examine the effects of bypass ratio principally on fuel economy. (Although the nacelle weight does not change at a fixed specific thrust, the effect of changing bypass ratio on the total weight of the engine is complicated. At fixed  $OPR$  and  $\hat{F}_N$ , increasing  $B$  implies higher  $T_{04}$ . Thus, in order to deliver the same net thrust, the size and weight of the core engine decreases while the weight of the LP system increases. Similarly there can be a subtle effect of changing bypass ratio on the bypass duct loss. It is probable that the relative amount of bypass duct loss ( $\Delta p_0/p_0$ ) decreases with increasing bypass ratio<sup>(11)</sup>.)

Calculations are carried out, using GasTurb, at different specific thrusts (representative of current and future possible designs) and the results are plotted in Fig. 6. Three sets of results are plotted for three values of the overall pressure ratio.

One can conclude from Fig. 6 that:

- (i) For each value of the specific thrust, there is a bypass ratio that gives the minimum specific fuel consumption. This is the optimum bypass ratio.

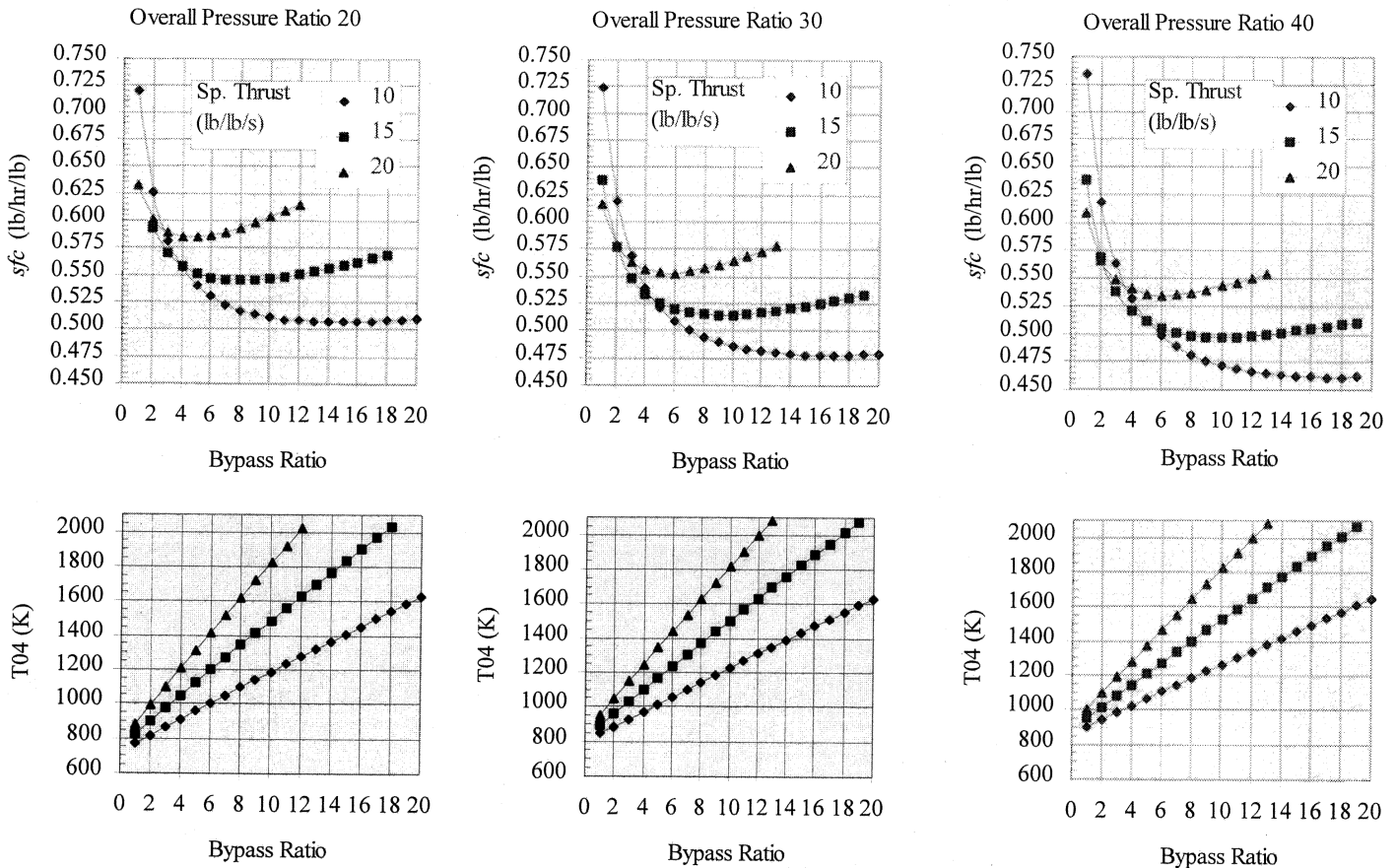


Figure 6. Effects of varying bypass ratio at constant specific thrusts. (Numerical calculations are carried at three levels of specific thrusts at three overall pressure ratios. The corresponding  $T_{04}$  are also plotted. At each point the fan pressure ratio is optimised. For all points, altitude = 11km,  $M = 0.82$ , isentropic efficiency of compressors and turbines = 0.9,  $Q_{cv} = 43.124 \text{ MJ/kg}$ ).

- (ii) The optimum bypass ratio increases with decreasing values of specific thrust. It depends only weakly on the overall pressure ratio.
- (iii) There is no value in employing any higher  $T_{04}$  than that at the optimum bypass ratio. (The value of  $T_{04}$  obtained by this method would be different from that determined from consideration of thermal efficiency of the core engine alone.)
- (iv) At low specific thrust level, the  $sfc$  versus  $B$  curves are sufficiently flat near the optimum value. One can therefore use significantly lower value of  $B$  than optimum, without appreciably increasing the  $sfc$ . This results in the use of lower  $T_{04}$ , which allows the thrust growth potential of the engine in the future with the minimum change. A lower bypass ratio reduces the number of LP turbine stages and may avoid the use of a gear drive.

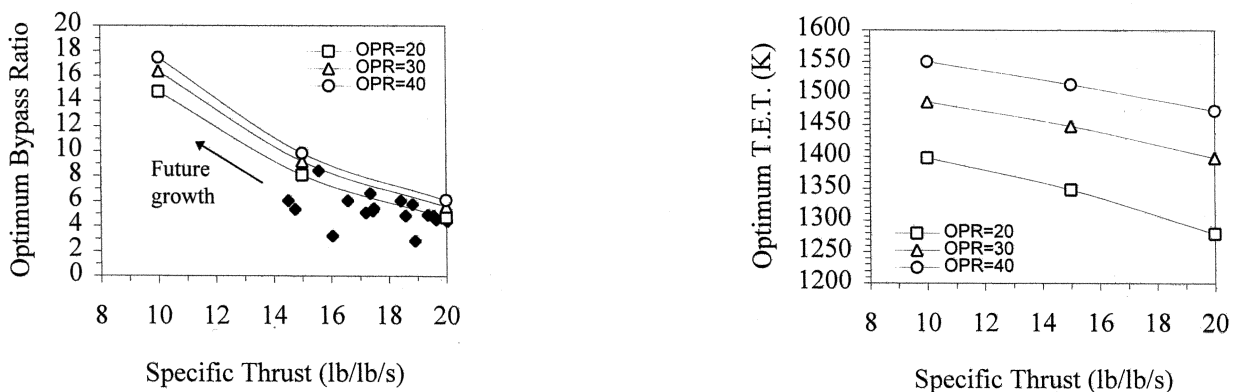


Figure 7. Optimum bypass ratio and optimum turbine entry temperature as a function of cruise specific thrust. (The filled symbols are data for current engines for civil transport. Calculations correspond to Fig. 6 which shows that, at low specific thrust level, adopting a slightly lower bypass ratio than optimum would not reduce  $sfc$  significantly but would reduce the TET considerably. For all optimisation calculations, altitude = 11km,  $M = 0.82$ , isentropic efficiency of components = 0.9).

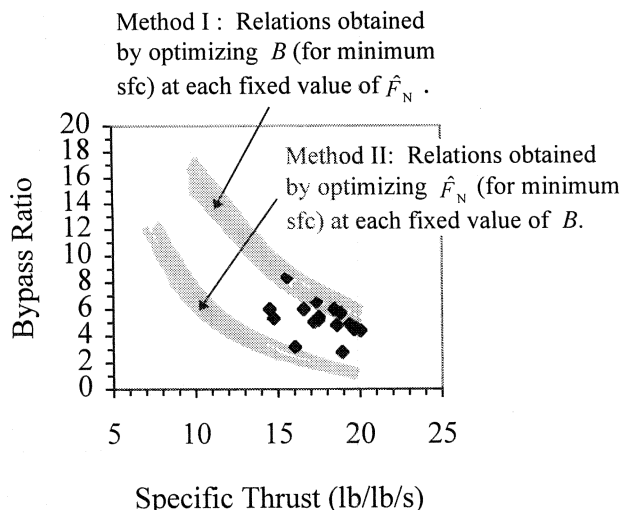


Figure 8. Relations between bypass ratio and specific thrust for two different optimisation processes. (Numerical calculations correspond to Fig. 7 and Appendix II. Thickness of the bands reflects various  $OPR$  in the range 20–40. Filled symbols are current civil engine data of various manufacturers. For all optimisation calculations, altitude = 11 km,  $M = 0.82$ , isentropic efficiency of components = 0.9).

- (v) The  $sfc$  versus  $B$  curves for various specific thrusts cross each other indicating that there is an optimum specific thrust if bypass ratio were kept fixed at a particular value. This topic has been discussed in Appendix II.

The computed variations of optimum bypass ratio with specific thrust are plotted in Fig. 7. Data of current civil engines are also plotted in the same figure for comparison. Figure 7 shows how the parameters should be varied for future high-bypass-ratio, low-specific-thrust engines. Figure 7 also shows the optimum turbine entry temperature as a function of specific thrust. As noted in point (iv) above, using slightly lower than optimum bypass ratios would not significantly deteriorate the  $sfc$ , but would reduce TET.

The existence of the optimum bypass ratio can be explained as follows. It has been mentioned in the Introduction that  $\eta_0 = \eta_p \eta_T$ .  $\eta_p$  is constant at a fixed specific thrust. So,  $\eta_0 \propto \eta_T$ . The thermal efficiency,  $\eta_T$ , does not just depend on  $OPR$ ,  $T_{04}$  and component efficiencies, as it does in a ground-based gas turbine. It also depends on the dissipation of mechanical energy in its transfer from the core to the bypass stream. One may write,

$$\eta_T = \eta_{core} F(B, \eta_{KE}, \hat{F}_N) \quad \dots (21)$$

A general expression for the transmission efficiency function  $F$  could be derived from equations (3), (7), (8) and (9).  $F$  can also be determined numerically (Appendix I) from calculations already performed to draw Fig. 6. The important properties of  $F$  are that it has a value of 1 when  $B = 0$ , and it decreases with increasing  $B$ . With increasing bypass ratio, a higher proportion of total energy is transferred to the bypass stream and thus the effect of the transmission loss becomes more important.

At fixed  $\hat{F}_N$  and  $OPR$ , an increase in  $B$  is accompanied by an increase in  $T_{04}$ , which raises  $\eta_{core}$ . This raises  $\eta_T$  initially. However, after the optimum value, any further increase in  $B$  makes  $\eta_T$  to decrease for two reasons:

- As  $B$  increases, the reduction in the value of function  $F$  counteracts the gain in  $\eta_{core}$ .
- Above a certain  $T_{04}$ ,  $\eta_{core}$  itself starts decreasing due to real gas effects. (This hitherto unreported effect, also to be expected in ground-based gas turbines, is explained by Guha<sup>(18)</sup>.)

## 5.0 OPTIMISATION AT FIXED SPECIFIC THRUST VERSUS OPTIMISATION AT FIXED BYPASS RATIO

The optimum relation between the bypass ratio and specific thrust can be determined in two different ways, as displayed in Figure 8. This comparison provides physical insight and puts the present method of optimisation in perspective.

The upper shaded area in Fig. 8 is a reproduction of the curves of Fig. 7(a). At chosen values of  $OPR$  and  $\hat{F}_N$ , the quantities  $B$ ,  $T_{04}$  and  $FPR$  are simultaneously optimised to give the maximum  $\eta_0$ , subject to the constraint that the value of  $\hat{F}_N$  remains fixed. This gives the optimum value of the bypass ratio,  $B_{op}$ . The same calculations are then repeated at various values of  $\hat{F}_N$  (and various levels of  $OPR$ ). This method is denoted as Method I. This is the recommended method of the present study as discussed in Section 4.0, fully depicted later in Fig. 12.

The lower shaded region in Fig. 8, on the other hand, represents the optimal relation between bypass ratio and specific thrust as calculated by Method II, fully described in Appendix II. This is the method recommended by Cohen *et al.*<sup>(4)</sup>. Walsh and Fletcher<sup>(7)</sup> (their Charts 6.19–6.25) use a combination of Cohen's method and single-variable parametric analysis. In Method II, at each fixed  $OPR$  and  $B$ ,  $T_{04}$  and  $FPR$  are optimised to achieve minimum  $sfc$ . The value of specific thrust at the point of minimum  $sfc$  calculated in this way is the optimum,  $(\hat{F}_N)_{op}$ , at the selected, fixed bypass ratio. The same calculations are then repeated at various values of  $B$  (and various levels of  $OPR$ ).

Method II seems to explore many possible combinations of  $OPR$ ,  $B$ ,  $T_{04}$  and  $FPR$ , and therefore could be thought to produce unique optimisation results. A comparison of Figs 6–8 and the data given in Appendix II, however, shows that, at any chosen value of specific thrust, Method II produces optimum solutions with lower  $B$ , lower  $T_{04}$  and higher  $sfc$  as compared to Method I. The relation  $\eta_0 = \eta_p \eta_T$  and Equation (21) can again be used to understand why this is so.

At a fixed  $B$ , increasing  $T_{04}$  increases specific thrust, which in turn decreases  $\eta_p$ . Figure A1 shows that at a fixed  $B$ , increasing specific thrust decreases the value of  $F$  slightly. At a fixed  $OPR$ , increasing  $T_{04}$  increases  $\eta_{core}$  until  $T_{04}$  is too high. Thus in Method II, the value of  $(\hat{F}_N)_{op}$  is obtained at that  $T_{04}$  at which the effect of increasing  $\eta_{core}$  is balanced (mainly) by that of decreasing  $\eta_p$ . The locus of minima in Fig. A3 is given by the condition  $d\eta_0/dT_{04} = 0$  which translates into  $1/\eta_{core} d\eta_{core}/dT_{04} \approx -1/\eta_p d\eta_p/dT_{04}$ . It is recalled from Section 4 that in Method I, this balance was obtained between  $\eta_{core}$  and  $F$  ( $\eta_p$  being constant) that determined the value of  $B_{op}$ . The condition  $d\eta_0/dB = 0$  translates into  $1/\eta_{core} d\eta_{core}/dB = -1/F dF/dB$  (Fig. 6 shows that  $B$  and  $T_{04}$  are almost linearly related in Method I). Since the variation in  $\eta_p$  in Method II is higher than the variation in  $F$  in Method I, the optimum condition is reached at a lower  $T_{04}$  in Method II.

It might be possible to determine  $B_{op}$  from Fig. A3 by examining the conditions at the envelope, though with considerable difficulty. This can only be performed graphically (with consequent limitation on accuracy) and the procedure is laborious as it needs the calculation and plotting of the whole set of data to construct an envelope. The determination of  $B_{op}$  by Method I at any particular value of specific thrust, as shown in Fig. 6, is direct and can be accomplished numerically.

To summarise, optimisation by keeping specific thrust fixed and varying bypass ratio gives different results from that by keeping bypass ratio fixed and varying specific thrust. This difference is shown in Fig. 8. The values corresponding to the current civil engines are also plotted in Fig. 8 for comparison. (Table 2 shows another example of the dependence of values of optimised quantities on the method of optimisation. Optimisation of a turbofan engine therefore requires extreme care; one needs to be clear about what is the full meaning when one uses an expression such as 'the optimum value of a variable'.)



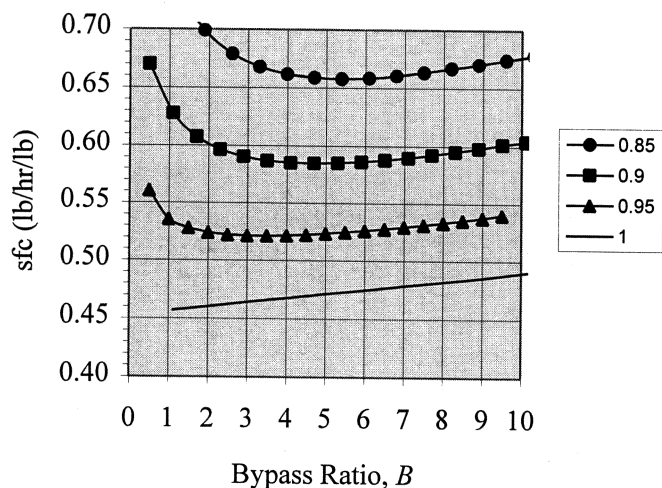


Figure 9. Effects of compressor and turbine isentropic efficiencies on optimum bypass ratio. (Calculations are carried out at fixed  $\dot{F}_N = 20 \text{ lb/lb/s}$ . For all calculations, altitude = 11 km,  $M = 0.82$ ,  $OPR = 20$ ,  $Q_{cv} = 43.124 \text{ MJ/kg}$ .  $FPR$  has been optimised at each point).

## 6.0 EFFECTS OF COMPONENT EFFICIENCIES ON THE OPTIMUM BYPASS RATIO

There is a continuous drive to improve the component efficiencies as much as possible. This is always beneficial and produces a marked improvement in gas turbine performance. (The designer also directs part of the improvement in aerodynamics to the reduction of number of stages, rather than to the improvement in isentropic efficiency. This reduces the weight of the engine and number of parts count.) Since the work ratio of the gas turbine thermodynamic cycle is rather poor, component losses have a disproportionate effect on the thermodynamic efficiency of the power plant. As the component efficiencies improve, the performance of the real engine approaches

that of the ideal Joule cycle. Figure 9 shows the effects of various component isentropic efficiencies on the optimum bypass ratio, calculated by using GasTurb.

The calculations shown in Fig. 9 were performed for an  $OPR = 20$ , and  $\dot{F}_N = 20 \text{ lb/lb/s}$ ; but the same trends are observed at other values of pressure ratio and specific thrust. The figure shows that as component efficiencies are improved, the optimum conditions occur at progressively lower bypass ratios. The limiting behaviour, when all components are ideal (i.e. isentropic), is interesting because it shows that  $sfc$  monotonically rises with bypass ratio. This means that, with ideal components, there would be no advantage in terms of fuel consumption in using a turbofan engine; the turbojet will be more economical even at subsonic speeds. However, bypass engines may still offer advantages in terms of weight reduction.

## 7.0 EFFECTS OF OVERALL PRESSURE RATIO ON SPECIFIC FUEL CONSUMPTION

The overall pressure ratio,  $OPR$ , is an important parameter. A study of the ideal Joule cycle shows that the thermal efficiency is a function of  $OPR$  alone and increases monotonically with  $OPR$ . When component losses are introduced in the analysis of a closed-circuit gas turbine plant producing shaft power<sup>(18)</sup>, it is found that (i) the actual thermal efficiency is significantly lower than the Joule cycle efficiency, and (ii) for each value of  $T_{04}$  (and component isentropic efficiencies) there exists an optimum pressure ratio above which any further increase in pressure ratio would decrease the thermal efficiency.

Often this idea is directly translated in descriptions of jet engines. However, it has been argued here that separate consideration of thermal and propulsive efficiency may lead to improper conclusions. It is for this reason that Fig. 10 plots the effects of changing  $OPR$  on the overall performance parameter, specific fuel consumption.

Variation in  $sfc$  with  $OPR$  may have been shown in some references but the speciality of the present approach arises from (i) the use of specific thrust as the basic parameter, (ii) the use of real gas properties, and (iii) the use of optimised values of the fan pressure ratio at each point of calculation.

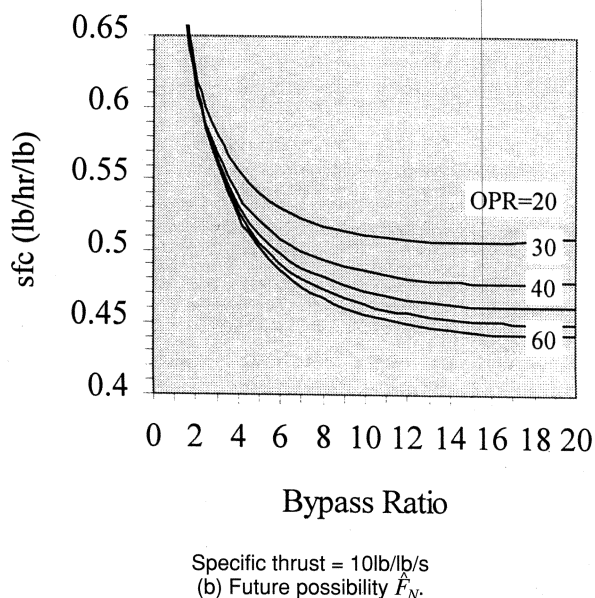
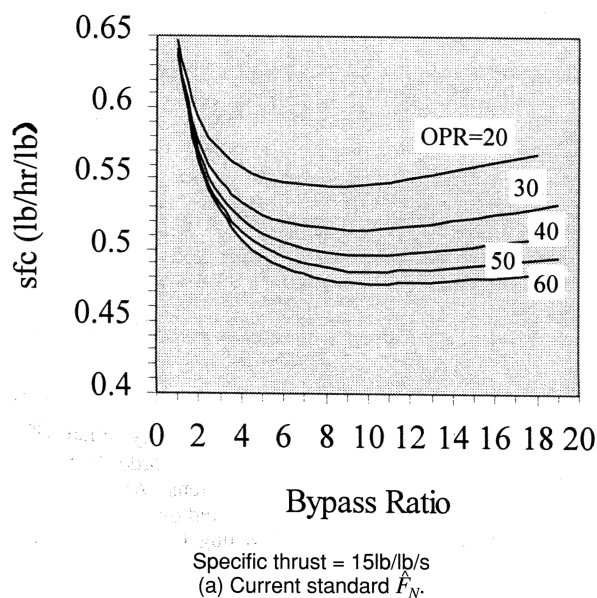


Figure 10. Effects of overall pressure ratio on specific fuel consumption. (For all calculations, altitude = 11 km,  $M = 0.82$ , isentropic efficiency of compressors and turbines 0.9,  $Q_{cv} = 43.124 \text{ MJ/kg}$ .  $FPR$  has been optimised at each point.  $T_{04}$  is different at each point as shown in Fig. 6).

Figure 10 shows two sets of graphs corresponding to two specific thrust levels. It can be seen that increasing *OPR* even up to 60 would continuously reduce the *sfc*.

Increasing *OPR*, however, causes other design problems. It would necessitate greater number of stages – increasing engine length, weight, cost and parts count. There is a limit to the attainable maximum pressure ratio (~6) from a multistage compressor on a single shaft for stable operation under off-design conditions. A three-spool configuration (as in RB211) or variable stators (as in GE90) may have to be used to alleviate this problem. Another limit comes from the allowable operating temperatures from stress considerations in rotating parts in the compressor. Higher pressure ratios result in higher temperatures: 870K is about the maximum that can be allowed with rotors made of titanium alloy, 990K for the nickel based alloy (which is heavier). Higher compressor delivery temperature also makes the cooling of HPT blades more difficult. Nevertheless, the *OPR* in 2010 is predicted to be around 40 for smaller engines and 55 for larger engines. Today's largest engines typically have an *OPR* of 40. The future marked increase in *OPR* would be due to higher component loading resulting from improved aerodynamic design and higher strength materials.

## 8.0 DIRECT ENGINEERING COST ANALYSIS TO DETERMINE THE OPTIMUM SPECIFIC THRUST

The aim of any engine manufacturer who wants to be competitive is to provide the lowest propulsion system cost to the airline. The engine performance is an important issue but also important are the acquisition cost, reliability and maintainability (and satisfying legislations). The industry has therefore always paid particular attention to cost studies<sup>(1,11,12,19)</sup>.

Overall, in civil engines, direct operating cost is optimised and in military engines, life cycle cost is optimised. Bennett<sup>(1)</sup>, Jackson<sup>(11)</sup> and Wilde<sup>(12)</sup> have shown that when the DOC is calculated at various specific thrusts, the resulting curves show a characteristic bucket-shape giving a particular value of specific thrust that minimises the DOC. The engine design, therefore, needs to be carried out at this optimum value of specific thrust. Jackson<sup>(11)</sup> has presented detailed considerations on the choice of specific thrust and Wilde<sup>(12)</sup> has described very detailed design issues.

There is an optimum specific thrust for any aircraft mission and technology standard. The optimum is a function not only of the gas path performance (e.g. the thermal efficiency of the core engine) but also depends on, among other things, installation losses, weight, engine price, fuel price, and effects on noise and mechanical considerations. Since some or all of these may vary with time, the determination of optimum specific thrust should be re-examined from time to time.

Full costing would require detailed knowledge about the engine and the required data might be proprietary information of engine manufacturers. However, information available in the public domain, eg the Association of European Airlines (AEA) parametrics, provides useful results. With this in view, Lee and McCaffer<sup>(20)</sup> have developed a model for calculating direct engineering costs (DEC) of various engines. This comprises:

- Engine price
- Nacelle cost
- Fuel cost over ten years
- Maintenance cost over ten years.

In order to find the optimum specific thrust, one also needs to include in the model,

- Cost of any increase in engine weight with decreasing specific thrust (this has to be balanced against the decrease in fuel weight due to improved *sfc*)
- Cost of any increase in drag with decreasing specific thrust.

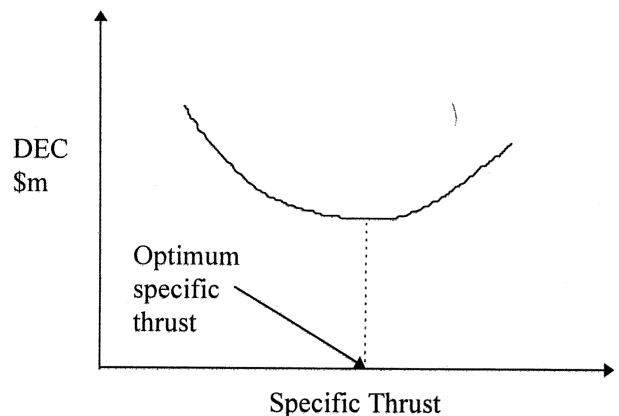


Figure 11. Direct engineering cost analysis to select the optimum specific thrust.

However, inclusion of these two factors might restrict the study to a particular aircraft-engine combination and the generic nature of the analysis would then be lost to some extent.

The optimum specific thrust (Fig. 11) would change with various requirements of overall thrust and aircraft range. This is so because the proportion of various elements to the overall cost changes depending on the overall thrust level, stage length etc. As the range decreases and engine size reduces, the relative proportion of maintenance costs increases, as the reliance is on number of flight cycles rather than flying time. For larger, long-range engines, fuel price assumes dominance. Legislation, such as stringent noise requirements, may also dictate the choice of specific thrust.

At lower specific thrusts and higher bypass ratios, new technology challenges have to be met. As the bypass ratio increases, the number of LPT stages may become unacceptably high and/or the limited bore size of the core engine may create mechanical and structural problems to the LP shaft. At bypass ratios higher than 10, a reduction gear would be necessary. The gearbox will probably find application in medium thrust range engines. The gearbox will add weight to the engine; moreover designing an efficient gear box transferring very high power is a challenging task (in spite of the high transmission efficiency of a gear, the rate at which heat needs to be removed from its oil may be substantial). High bypass ratio may reduce the size of the core engine to such an extent that the component efficiencies may deteriorate. This degradation is caused by offset flow path and curved duct between the fan and core compressor inlet, the relatively high hub-tip ratio of the high pressure compressor and turbine with their performance sensitivity to blade tip clearance losses, the difference in diameters and blade speeds of the LP and HP turbines compromising the aerodynamic designs and introducing additional losses in the duct and LP nozzle between the two turbines<sup>(12)</sup>.

Low specific thrust engines offer challenges in installation both from geometric constraints and interference drag points of view. The optimum *FPR* decreases with decreasing specific thrust. Below an *FPR* of 1.4, the engine will require variable geometry either via a variable pitch fan or a variable area bypass nozzle in order to provide aerodynamic stability under off-design conditions. At still lower specific thrust, one may have to employ advanced ducted propulsors (ADP), perhaps in the form of counter-rotating fans. At such low specific thrust, the nacelle length may have to be reduced to decrease drag and weight penalty. However, this could make the fan noise a problem. At specific thrust lower than 5lb/lb/s, the nacelle may have to give way altogether – an unducted propfan could be used. Cabin noise, fan blade containment and installation problems are the stumbling block for unducted propulsors.



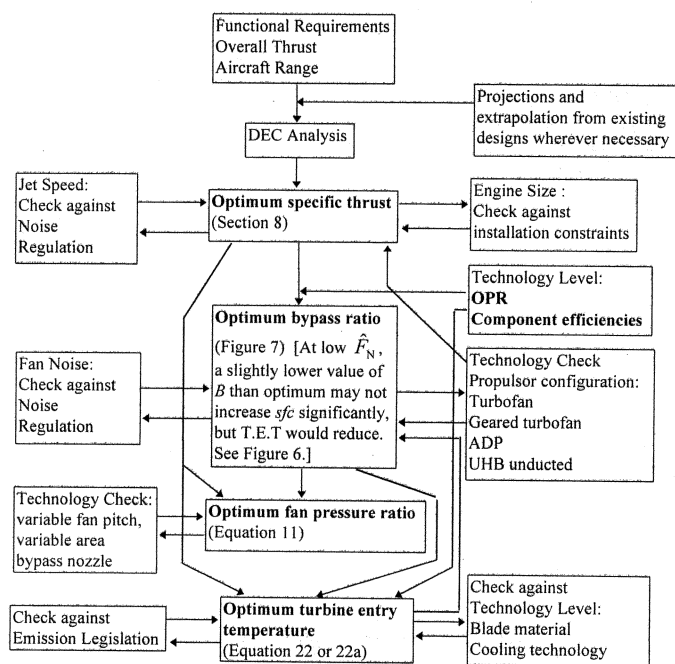


Figure 12. Schematic diagram for the (numerical or analytical) determination of optimum parameters.

## 9.0 OVERALL OPTIMISATION METHODOLOGY

Figure 12 schematically shows the various steps involved in the present thermodynamic optimisation process. Once the specific thrust,  $OPR$  and bypass ratio are known, the optimum turbine entry temperature is fixed and can be calculated. An accurate calculation can be involved, particularly to include the real gas effects<sup>(21)</sup>. However, an approximate equation for  $T_{04}$  can be written, by considering the energy transfer processes, as

$$\frac{T_{04}}{T_a} \left[ 1 - (OPR)^{\frac{1-\gamma}{\gamma}} \right] \eta_t = \frac{\gamma-1}{2} (1+B) \left[ \eta_c \left( \frac{\hat{F}_N}{\sqrt{\gamma R T_a}} + M \right)^2 - \eta_c M^2 \right] + \frac{1}{\eta_c} \left[ (OPR)^{\frac{\gamma-1}{\gamma}} - 1 \right] \quad \dots (22)$$

where,  $\eta_c$  and  $\eta_t$  are the isentropic efficiencies of the compressor and turbine respectively. Equation (22) shows that, for fixed  $OPR$  and  $\hat{F}_N$ ,  $T_{04}$  varies linearly with bypass ratio  $B$ . Figure 6, calculated by GasTurb, shows that this behaviour is approximately true.

The accuracy of Equation (22) is tested against numerical optimisation performed by GasTurb and the results are shown in Fig. 13. The calculations are shown for  $OPR = 40$ , but similar results are obtained at other pressure ratios. Results for two values of specific thrusts ( $\hat{F}_N = 20 \text{ lb/lb/s}$  and  $\hat{F}_N = 10 \text{ lb/lb/s}$ ) are plotted as these cover the range of current designs and future possibilities. A wide range of bypass ratios is shown, the optimum value of which can be read from Fig. 6. Figure 13 shows that, over the entire range of specific thrust, Equation (22) performs rather well in comparison with numerically optimised results. The agreement becomes almost perfect, if a small empirical correction is added to Equation (22), remembering that the numerical results use real gas properties including dissociation:

$$T_{04} = T_{04, \text{Equation (22)}} + 5 \left[ 100 / \hat{F}_N, (\text{lb/lb/s}) - B \right] \quad \dots (22a)$$

The empirical correction in Equation (22a) remains valid over the range of specific thrust,  $B$  and  $OPR$  suitable for current and future designs.

Cumpsty<sup>(5)</sup> has shown how the turbine entry temperature has increased progressively and significantly over the last 50 years. Over the last 20 years there has been an average increase of about 8K per year in turbine entry temperature. It seems that engine manufacturers will try to maintain this trend in the foreseeable future with improved cooling technology and material. (Bennett<sup>(1)</sup> shows that at the same cooling technology level an increase in TET at take-off from 1,550K to 1,700K results in almost no improvement in core thermal efficiency. With improvement in cooling technology, with constant percentage cooling air flow, the same temperature rise gives about 2% improvement in core thermal efficiency. With ceramics, with no cooling air, the improvement will be 6%.) It is predicted that in 2010 the maximum permissible TET at take-off would exceed 1,900K.

There seems to be a widespread belief that 'higher the TET, better would be the performance', i.e. one should employ the highest possible TET that the technology would permit. Figures 6, 7 and 13, on the other hand, show that engines with different specific thrusts, pressure ratios and bypass ratios would need different TETs which have to be calculated. (Analogy with land-based gas turbines may also lead to difficulty. For shaft-power producing plants, at any constant pressure ratio with perfect gas, higher the TET, higher is the thermal efficiency<sup>(18)</sup>. The effect of increased TET on fuel consumption in a jet engine is complex because higher TET may result in higher jet velocity which reduces propulsive efficiency. Figure A2 shows that the thermal efficiency decreases above the optimum TET. The main effect of increased TET in a jet engine is that it increases specific core power reducing the core engine size.) High TET is bad for turbine blade life due to creep and thermal fatigue. It is therefore important not to use any higher than the optimum value both from performance and maintenance point of view.

In the present methodology, once the optimum specific thrust is determined from DEC analysis (Section 8), and  $OPR$  and isentropic efficiencies (at affordable technology level) are chosen, Fig. 7, Equation (11) and Equation (22) quickly give the optimum values of  $B$ ,  $FPR$  and  $T_{04}$  that would minimise  $sfc$ . This analytical procedure, therefore, gives hand calculations almost the same power and accuracy as sophisticated computer programs at the initial phase of design.

It should be realised, however, that for the final realistic solutions, one has to resort to detailed computation involving turbine blade cooling, bleed, power offtake, and loss modelling. For example, the influence of bypass duct loss on  $sfc$  in a low specific thrust engine may be significant. Moreover, optimisation taking component

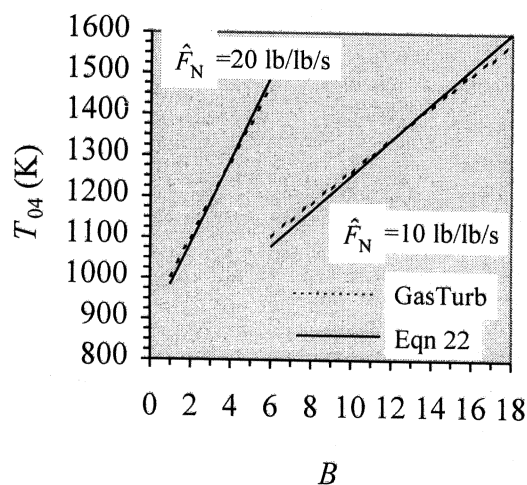


Figure 13. Comparison of the prediction of Equation (22) with numerical optimisation results from GasTurb. (For all calculations, altitude = 11km,  $M = 0.82$ ,  $OPR = 40$ , isentropic efficiencies of compressors and turbines 0.9.  $FPR$  has been optimised at each point).

designs into account would result in slightly different values of the parameters from those determined considering the overall cycle alone. Similarly an engine should be optimised together with the aircraft including various requirements such as those during takeoff, climb and landing. Realistic optimisation should consider the recursive effects of the previous stage of design on the values of the parameters used for the optimisation (for example, the effect of high bypass ratio on component efficiencies of the core engine). The scheme shown in Fig. 12 can be used also for numerical optimisation in which the optimum bypass ratio, fan pressure ratio and turbine entry temperature are determined simultaneously.

At many places in the paper, several design constraints on various parameters and the effects of off-design performance have been indicated. These may lead one to choose values different from the thermodynamic optimum. From engine manufacturers' point of view, there are also practical constraints in adopting a 'clean-sheet analysis'. They may be inherently restricted by previous program investment and consequently only consider development of their current product range and in-house technologies. The strategy to design a small number of engine architectures, that allow scaling of both the fan and the core size to produce a range of engines, reduces the unit production cost. Ruffles<sup>(9)</sup> describes how successful the Trent and RB211 engines have been by adopting a philosophy of scaled modules with shared technology and experience to deliver thrust from 40,000lbf to over 100,000lbf (the Trent family covers most of this thrust range with only two fan diameters of 97.5 and 110in). If manufacturers' current drive to significantly reduce the product development time and cost succeeds, and the fuel cost increases, then the case for turbofan engines with lower specific thrust or new engine concepts may become compelling.

A modern turbofan engine is a complex object and its design involves many aspects. The designer has to consider not only the aero-thermodynamic performance of its internal gas path but also the mechanical design, manufacturing, installation, weight, cost, noise, reliability and maintainability. A summary of the success of the industry in the evolving design of jet engines has been mentioned in the Introduction.

## 10.0 CONCLUSION

A systematic methodology for the thermodynamic optimisation of bypass engines – turbofan or advanced propulsors – is presented (Fig. 12). The process starts with establishing an optimum specific thrust for the engine based on an economic analysis (installation constraints, noise regulations etc. also need to be considered). The task of the optimisation process is then to find the combination of optimum values of  $OPR$ ,  $B$ ,  $FPR$  and  $T_{04}$  concurrently that maximises the overall efficiency at the fixed specific thrust.

Figure 7, Equation (11) and Equation (22) can quickly establish these optimum values of  $B$ ,  $FPR$  and  $T_{04}$ . The derived analytical relations are simple and explicit, and compare well with numerical optimisation using real gas properties performed by the specialist computer package GasTurb (Figs 4, 5 and 13). This analytical procedure, therefore, gives (the simpler and quicker) hand calculations almost the same power and accuracy as sophisticated computer programs. The analytical relations not only accelerate the optimisation process but also offer physical insight. The scheme, depicted in Fig. 12, and the theory should make it possible to treat the optimisation of turbofan engines realistically within the scope of a textbook.

The usual parametric studies, eg those given in many standard texts, involve the numerical calculation of engine performance as a single parameter is varied each time, while keeping all other parameters fixed – therefore not at their optimum values. Parametric studies with a single variable are inadequate in finding true optimum conditions in jet engine design (even if they produce the typical 'U-shaped' curves). Moreover, such parametric studies may be associated with large excursions in the value of the specific thrust which

is not acceptable for real design. The scheme shown in Fig. 12 avoids both difficulties.

The effects of various parameters on the performance of the engine have been presented systematically. For example, Fig. 6 shows the variation of  $sfc$  with bypass ratio at fixed  $\dot{F}_{N_s}$ , Fig. 9 shows the effects of component isentropic efficiencies on optimum bypass ratio, Fig. 10 shows the effects of overall pressure ratio on  $sfc$ . The choice of specific thrust as the fundamental parameter helps in realistic interpretation of the results. The calculated results shown in various figures correspond to a range of specific thrust suitably chosen to reflect the current and future design standards.

In the context of a bypass engine the use of the word 'optimum' needs care; Fig. 8 and Table 2 explain this point. Figure 8 shows that optimisation by keeping specific thrust fixed and varying bypass ratio gives different results from that by keeping bypass ratio fixed and varying specific thrust (if  $\dot{F}_{N_{op}}$  is the optimum specific thrust at a fixed bypass ratio  $B$ , then the same  $B$  is not the optimum bypass ratio at the particular value of specific thrust  $\dot{F}_{N_{op}}$ ).

Equation (18) gives the variation in optimum jet speed ratio as a function of bypass ratio. Figure 5 shows that it compares well with numerical optimisation results. This resolves the difficulties with earlier theories which predicted a constant jet speed ratio at any bypass ratio.

Present investigation has established the existence of an optimum bypass ratio which has not been reported previously (Section 4, Figs 6 and 7). It has been shown that the optimum bypass ratio increases with decreasing specific thrust, decreases with improved component efficiencies and weakly depends on overall pressure ratio. The reasons for its existence have been explained by Equation (21), elaborated in Appendix I. This is a true thermodynamic optimum as at each point of calculation the optimum combination of different values of  $FPR$  and  $T_{04}$  has been used (see Fig. 6). Previous issues such as increased nacelle drag with increasing bypass ratio (see second paragraph in Section 4) do not arise here because the optimisation has taken place at a fixed specific thrust, thus giving the concept of optimum bypass ratio an unambiguous meaning. The existence of the optimum bypass ratio also means that there is an optimum TET above which any further increase would deteriorate the  $sfc$ . The optimum TET can be determined from Fig. 7 or can be calculated from Equation (22a) by substituting the optimum value of bypass ratio in it.

The direct use of overall efficiency in describing fuel economy is advocated here. Several examples have been mentioned where its much-used decomposition into thermal and propulsive components may cause difficulty. Appendix I, in particular, shows the numerically calculated variation of an often-forgotten parameter – the transmission efficiency function  $F$ . It is shown that this, together with real gas effects, is responsible for establishing the optimum value of bypass ratio. The optimum turbine entry temperature determined from the considerations of core thermal efficiency alone (in analogy to ground based gas turbines) would be different from the optimum values determined in this paper by maximising the overall efficiency. (Ref. 18 explains the role of real gas behaviour in establishing the optimum turbine entry temperature.)

The proposed optimisation scheme, as shown in Fig. 12, can also be used for numerical computation which must be adopted in the final phase of design when inclusion of turbine blade cooling, bleed, power offtake, losses in ducts and other passages, component design and other fine scale tuning are necessary.

The method presented here can be used for the design either of engines at the current specific thrust levels or of future low specific thrust, high bypass ratio engines.

## ACKNOWLEDGEMENTS

I am grateful to the first referee for boosting my morale by giving the paper the highest recommendation in all eight categories of eval-

uation and writing kind words. I am also grateful to the second referee, manifestly having industrial experience and expertise, for detailed suggestions to improve the clarity of the paper. I am fortunate to have N.A. Mitchell as a colleague who has a wealth of experience from his previous working life in aero-engine industry. A brief internal report of an aircraft manufacturer, entitled 'optimum jet velocity' and communicated by M. Smith, increased my drive to derive my own solution to this question. Gratitude to all previous authors and to whoever has helped me to learn.

## REFERENCES

1. BENNETT, H.W. Aero engine development for the future, proceedings of the Institution of Mechanical Engineers, July 1983, series A, **197**, pp 149-157.
2. RÜD, K. and LICHTFUSS, H.J. Trends in aero-engines development, aspects of engine airframe integration for transport aircraft, proceedings DLR Workshop DLR-Mitteilung, 6-7 March 1996, Braunschweig, Germany.
3. HILL, P.G. and PETERSON, C.R. *Mechanics and Thermodynamics of Propulsion*, 2nd edition, Addison-Wesley, Massachusetts, 1992.
4. COHEN, H., ROGERS, G.F.C. and SARAVANAMUTTOO, H.I.H. *Gas Turbine Theory*, 4th edition, Addison-Wesley Longman, London, 1996.
5. CUMPSTY, N.A. *Jet Propulsion*, CUP, Cambridge, 1997.
6. MATTINGLY, J.D. *Elements of Gas Turbine Propulsion*, McGraw-Hill, New York, 1996.
7. WALSH, P.P. and FLETCHER, P. *Gas Turbine Performance*, Blackwell, Oxford, 1998.
8. MEECE, C.E. Gas turbine technologies of the future, International Symposium on Airbreathing Engines (ISOABE), Melbourne, Australia, September 1995.
9. RUFFLES, P.C. The future of aircraft propulsion, proceedings of Institution of Mechanical Engineers, Part C, *J of Mechanical Engineering Science*, 2000, **214**, (C1), pp 289-305.
10. BIRCH, N.T. 2020 vision: the prospects for large civil aircraft propulsion, *Aeronaut J*, August 2000, **104**, (1038), pp 347-352.
11. JACKSON, A.J.B. Some future trends in aero engine design for subsonic transport, Transactions of American Society of Mechanical Engineers, *J of Engineering for Power*, April 1976, **98**, pp 281-289.
12. WILDE, G.L. Future large civil turboprops and powerplants, *Aeronaut J*, July 1978, **82**, pp 281-299.
13. Rolls-Royce Aero Data, TS 1491 Issue 9, Derby, 1991.
14. CLOFT, T.G., and MULDOON, P.L. Ultra high bypass (UHB) engine critical component technology, ASME paper 89-GT-229, 1989.
15. KURZKE, J. Manual for GasTurb 7.0 for Windows, 1996.
16. GUHA, A. Optimum fan pressure ratio for bypass engines with separate or mixed exhaust streams, revised version submitted to AIAA *J Propulsion and Power*, 2001.
17. SMITH, M. Optimum jet velocity, personal communication, 1999.
18. GUHA, A. Performance and optimisation of gas turbines with real gas effects, proceedings of the Institution of Mechanical Engineers, Series A, *J of Power and Energy*, 2001 (in press).
19. YOUNGHANS, J.L., DONALDSON, R.M., WALLACE, D.R., LONG, L.L. and STEWART, R.B. Preliminary design of low cost propulsion systems using next generation cost modelling techniques, *ASME J Engineering for Gas Turbines and Power*, Jan 1999, **121**, pp 1-5.
20. LEE, J.L. and MCCAFFER, M.A. Future High-Bypass Ratio Engines, MEng Report No 870, Department of Aerospace Engineering, University of Bristol, 1999.
21. GUHA, A. An efficient generic method for calculating the properties of combustion products, proceedings of the Institution of Mechanical Engineers, series A, *J of Power and Energy*, 2001, **215**, (A3), pp 375-387.

## APPENDIX I: THE VARIATION OF THE TRANSMISSION EFFICIENCY FUNCTION $F$ IN EQUATION (21)

Figure A1 shows the variation of  $F$  with bypass ratio, obtained numerically. The data correspond to the calculations shown in Fig. 6.  $F$  varies slightly with the specific thrust. It is found that the depen-

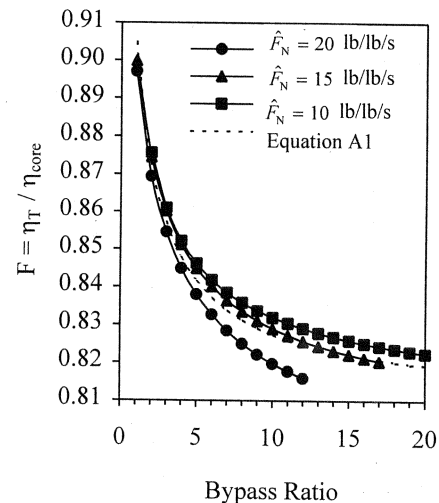


Figure A1. Variation in the transmission efficiency function  $F$ . (For all calculations, altitude = 11 km,  $M = 0.82$ ,  $OPR = 20-40$ . Isentropic efficiency of compressors and turbines 0.9, hence  $\eta_{KE} = 0.81$ . The lines containing filled symbols are determined numerically and correspond to Fig. 6).

dence of  $F$  on  $OPR$  (at fixed  $B$  and  $\hat{F}_N$ ) is negligibly weak. However, the thermal efficiency of the core engine,  $\eta_{core}$ , depends on  $OPR$ . This explains why the optimum bypass ratio depends, to some extent, on  $OPR$ , as shown in Fig. 7.

Bennett<sup>(1)</sup> provides a simple relation for  $F$ ,

$$F \approx \frac{1 + B\eta_{KE}}{1 + B} \quad \dots (A1)$$

Equation (A1) is also plotted on Fig. A1. The simple relation performs reasonably well, although it does not capture the variation in  $F$  with  $\hat{F}_N$ . To the knowledge of the present author, actual values of  $F$  determined by accurate numerical calculations (such as Fig. A1) have not previously appeared in the literature. The present paper has established that the variation of the function  $F$ , together with the variation of  $\eta_{core}$  considering real gas effects, plays a crucial role in determining optimum levels of bypass ratio and TET. Fig. A2 shows a typical variation in  $\eta_{core}$  and  $\eta_T$ . Further discussion on the variation of  $\eta_{core}$  can be found in Ref. 18.

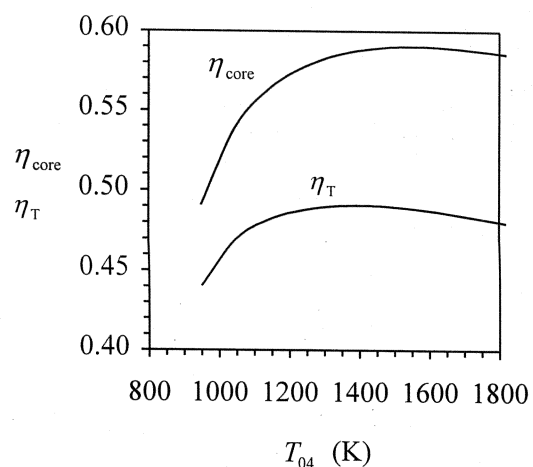


Figure A2. A typical variation in  $\eta_{core}$  and  $\eta_T$ . ( $\hat{F}_N = 20$  lb/lb/s,  $OPR = 30$ , isentropic efficiency of components 0.9. Calculations correspond to Fig. 6).

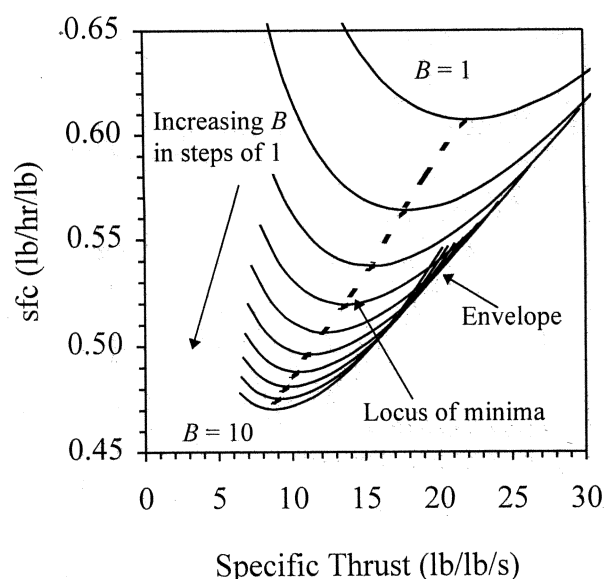


Figure A3. Optimisation results at fixed bypass ratios. (For all calculations, altitude = 11km,  $M = 0.82$ ,  $OPR = 40$ . Isentropic efficiency of compressors and turbines = 0.9.  $FPR$  has been optimised at each point).

## APPENDIX II: OPTIMISATION AT FIXED BYPASS RATIOS

Cohen *et al.*<sup>(4)</sup> (pp 112-114) have recommended this method of optimisation of a turbofan engine. They only present the method in outline. This appendix gives the quantitative optimisation results using GasTurb.

Each bucket-shaped curve in Fig. A3 is calculated by the following method.  $OPR$  and  $B$  are kept fixed. At the start of calculation, a set minimum value for  $T_{04}$  is chosen. The optimum fan pressure ratio is calculated for the selected combination of  $OPR$ ,  $B$  and  $T_{04}$  that minimises  $sfc$ .  $\dot{F}_N$  and  $sfc$  are calculated for the combination of  $OPR$ ,  $B$ ,  $T_{04}$  and  $FPR_{op}$ , and plotted on Fig. A3. Keeping  $OPR$  and  $B$  fixed,  $T_{04}$  is increased in small steps (until a set maximum value is reached) and the previous procedure is repeated.

When calculations for a particular  $B$  are complete, the whole process is repeated for another value of  $B$ . Figure A3 shows the results for ten such calculations. Table 3 shows the values of various parameters at the point of minima for each curve.

Figure A3 shows the results for an  $OPR$  of 40. Similar figures can be drawn at other values of  $OPR$ . The optimum relations between the bypass ratio and specific thrust, as determined by the locus of minima, have been plotted in Fig. 8, covering a range of  $OPR$  20-40. Section 5 contains other relevant material.

**Table 3**  
Various optimised quantities corresponding to locus of minima in Fig. A3

Bypass ratio	$OPR$	Optimum $T_{04}$ (K)	Optimum $FPR$	Optimum $\dot{F}_N$ (lb/lb/s)	$sfc$ (lb/hr/lb)
1	40	1024.6	1.991	22.11	0.6071
2	40	1057.9	1.784	17.89	0.5638
4	40	1112.6	1.586	13.83	0.5194
6	40	1143.5	1.459	11.28	0.4962
8	40	1173.3	1.389	9.79	0.4812
10	40	1199.2	1.341	8.73	0.4705